New Insights from a Fixed Point Analysis of Single Cell IEEE 802.11 WLANs

Anurag Kumar, Eitan Altman, Daniele Miorandi, Munish Goyal

INRIA

INSTITUT NATIONAL DE RECHERCHE EN INFORMATIQUE ET EN AUTOMATIQUE

New Insights from a Fixed Point Analysis of Single Cell IEEE 802.11 WLANs

Anurag Kumar — Eitan Altman — Daniele Miorandi — and Munish Goyal

N° 5218

June 2004

Thème COM

ISSN 0249-6399 ISRN INRIA/RR--5218--FR+ENG

New Insights from a Fixed Point Analysis of Single Cell IEEE 802.11 WLANs*

Anurag Kumar† , Eitan Altman‡ , Daniele Miorandi§ , and Munish Goyal¶

Thème COM — Systèmes communicants
Projet Maestro

Rapport de recherche n° 5218 — June 2004 — 38 pages

Abstract: We study a fixed point formalisation of the well known analysis of Bianchi. We provide a significant simplification and generalisation of the analysis. In this more general framework, the fixed point solution and performance measures resulting from it are studied. Uniqueness of the fixed point is established. Simple and general throughput formulas are provided. It is shown that the throughput of any flow will be bounded by the one with the smallest transmission rate. The aggregate throughput is bounded by the reciprocal of the harmonic mean of the transmission rates. In an asymptotic regime with a large number of nodes, explicit formulas for the collision probability, the aggregate attempt rate and the aggregate throughput are provided. The results from the analysis are compared with *ns2* simulations, and also with an exact Markov model of the back-off process. It is shown how the saturated network analysis can be used to obtain TCP transfer throughputs in some cases.

Key-words: IEEE802.11, Performance evaluation, Fixed point equation, wireless networks, CSMA/CA, performance of MAC protocols

* This work was supported by the Indo-French Centre for Promotion of Advanced Research (IFCPAR) under research contract No. 2900-IT.

† ECE Department, Indian Institute of Science, Bangalore, INDIA
‡ INRIA, Sophia-Antipolis, FRANCE
§ INRIA, Sophia-Antipolis, FRANCE
¶ ECE Department, Indian Institute of Science, Bangalore, INDIA

Unité de recherche INRIA Sophia Antipolis
2004, route des Lucioles, BP 93, 06902 Sophia Antipolis Cedex (France)
Téléphone : +33 4 92 38 77 77 —Télécopie : +33 4 92 38 77 65

Nouvelles perspectives d'une analyse de point fixe d'une seule cellule de WLANs IEEE 802.11

Résumé : Nous étudions une formulation d'un point fixe de l'analyse connue de Bianchi. Nous proposons une simplification considérable et généralisons l'analyse. Nous étudions dans ce cadre plus général, la solution du problème de point fixe ainsi que les mesures de performances qui en découlent. Nous démontrons l'unicité de la solution du problème de point fixe. Des formules simples et générales du débit sont obtenues. Nous montrons que le débit d'un flux quelconque est borné par le taux de transmission le plus petit. Le débit aggrégé est borné par l'inverse de la moyenne harmonique des taux de transmissions. Dans le régime asymptotique d'un grand nombre de nœuds (mobiles), nous obtenons des formules explicites pour la probabilité de collision, le taux aggregé de tentatives de transmission et du débit aggrégé. Les résultats de l'analyse sont comparés aux simulations par ns2 et aussi par une approche markovienne exacte du processus de *back-off*. Nous montrons comment l'analyse du réseau saturé peut être utilisé pour fournir le débit de connexions TCP dans certains cas.

Mots-clés : IEEE802.11, Évaluation de performances, Équation point fixe, CSMA/CA, Réseaux sans fil

1 Introduction

We consider wireless local area networks that use the IEEE 802.11 standards for physical transmission and medium access control (MAC) (see [8] for a concise description of these standards and some planned extensions). In particular, we are concerned in this paper with the network architectures depicted in Figure 1. There are several nodes within such a distance of each other that only one transmission can be sustained at any point of time. We call these *single-cell* networks (see Figure 1). Our discussion covers networks of both the types shown in the figure, i.e., *ad hoc networks* in which there is no central access point (AP) through which all traffic must pass, or *infrastructure networks* in which an AP acts as a conduit between the wireless network and a wired "infrastructure." In addition, in this paper our analysis is limited to the situation in which all nodes use the RTS/CTS based distributed coordination function (DCF) without the QoS extensions (as in IEEE 802.11e) (but see [9] for our extensions of the work in the present paper).

There are several *nodes*, each of which may have several physical *connections or associations* with several other nodes. On each such connection the sustainable *physical* transmission rate may be different. The physical layer definitions in the IEEE 802.11 standard support multiple transmission rates, and the standard includes mechanisms that permit nodes to agree on a transmission rate that performs well between them. Between each such pair of nodes there are *flows* whose throughput performance we are concerned with. It is assumed throughout this paper that all flows are infinitely back-logged at their transmitters; i.e., there are always packets to transmit when a node gets a chance to do so.

In such a scenario, we are interested in obtaining quantitative formulas and qualitative insights via a stochastic analysis of the way that the IEEE 802.11 CSMA/CA protocol

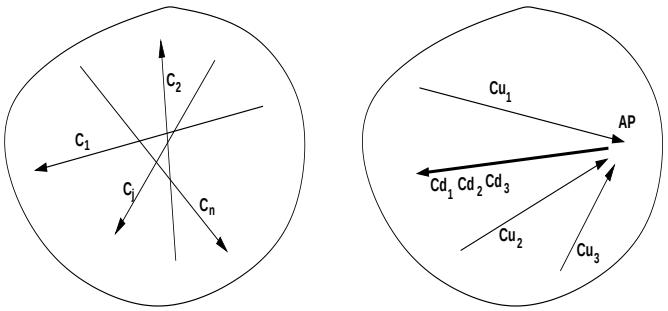

Figure 1: Single cell IEEE 802.11 networks; the one on the left is in the ad hoc mode, and the one on the right is in the infrastructure mode, with the AP serving as the access to a wired network. In the left panel C_i are the achievable physical transmission rates on the corresponding connections. In the right panel C_{u_i} refer to "up-link" transmission rates, and C_{d_i} refer to "down-link" transmission rates. In the IEEE 802.11 standard a receiver and a transmitter agree on a common physical transmission rate.

allocates the wireless medium to the node transmitters. Our approach is to begin with a key approximation made by Bianchi [3]. This leads to a fixed point equation, which can be expected to characterise the operating points of the system. This fixed point equation is our point of departure. We simplify and generalise the analysis leading to the fixed point equation. We then establish a simple, and practically appealing, condition for the uniqueness of the fixed point in this more general framework. Some simple observations lead to throughput formulas for the overall network and for the individual flows. These formulas allow us to recover the well known observation that the slowest transmission rate dominates the throughput performance. We also analyse the fixed point in the asymptotic regime of a large number of nodes and find explicit formulas for the collision probability, the channel access rate and the network throughput. A key parameter in the protocol is the back-off multiplier, whose default value in the IEEE 802.11 MAC standard is 2; we numerically study how the back-off multiplier affects the throughput.

We provide *ns2* simulation results for the collision probabilities and throughputs and compare these with results obtained from the fixed point analysis. We also provide results from an exact Markov chain model for the back-off process and also compare these results with those from the fixed point analysis.

As already pointed out, the above described modeling assumes that there are always packets backlogged on every connection. Such a *saturation assumption* is a common simplification and is useful in the following ways. In some situations it has been formally proved (see, for example, [6]) that the saturation throughput provides a sufficient condition for stability of the queues; i.e., if at each queue the arrival rate is less than the saturation throughput then the queues will have a proper, joint stationary distribution. In this paper we also apply the saturation throughput analysis to provide an analysis for TCP controlled file transfer throughputs in certain local area network scenarios.

Modeling and analysis of wireless networks is extremely important as, in addition to providing performance results, it helps to understand the strengths and limitations of the evolving protocols and standards. The role of such modeling in interpreting experimental results and in checking simulation outputs cannot be over-emphasised. The most popular model for IEEE 802.11 networks, and one that has led to many applications and extensions, is the one reported in [3]. Another analysis, that also incorporates the feature of adapting the back-off parameters, has been reported in [4]. The recent paper [2] is one of the many that have reported a throughput "anomaly" in IEEE 802.11 networks; i.e., if the network has low speed connections, even the high speed connections experience throughput no better than what is obtained by the low speed connections.

The paper is organised as follows. In Section 2 we provide the key observation and approximation on which the analysis is based. In Section 3 we analyse the back-off process in a fairly general setting. The fixed-point equation is provided in Section 4 and analysed in Section 5. In Section 6 the throughput formulas are provided. The asymptotic analysis is developed in Section 7. The longer proofs are in the Appendix.

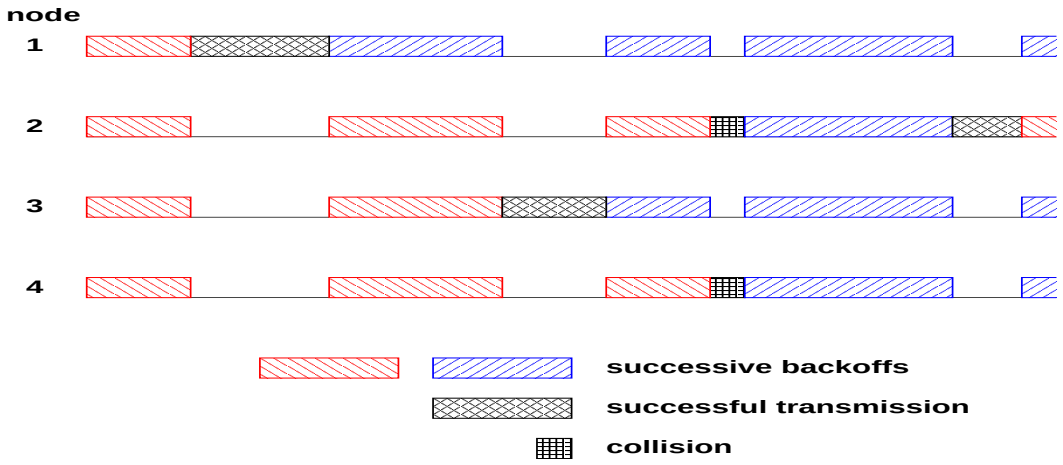

Figure 2: The evolution of the back-off periods and channel activity for four nodes. It can be seen that back-offs are interrupted by channel activity, i.e., packet transmissions and RTS collisions.

2 A Key Observation and an Approximation

2.1 Sufficient to Analyse the Back-Off Process

We begin by extracting from a description of the system the key modeling abstractions that will allow us to develop the analysis. Figure 2 shows the evolution of the system for 4 nodes; shown are the back-offs, the transmissions and collisions. In the IEEE 802.11 standard, the back-off durations are in multiples of a standardised time interval called a *slot* (e.g., 20 μs in IEEE 802.11b). However, this discrete nature of the back-offs does not affect the following argument. When a node completes its back-off (for example, node 1 is the first to complete its back-off in Figure 2), it seeks a reservation of the channel by sending an RTS packet. If no other node completes its back-off before hearing this transmission then the RTS effectively reserves the channel for the first node. There follows a CTS from the intended recipient of the RTS, and then there follows a packet transmission and a MAC level ACK. This ends the reservation period and the node that transmitted the packet samples a new back-off interval. Note that we assume throughout that nodes always have packets to transmit; i.e., *all the transmission queues are saturated.*

If the RTS collides with that of another node, then after fully transmitting their RTSs each node waits for a time interval DIFS before returning to the back-off state. For example, in Figure 2 nodes 2 and 3 collide after the first two attempts (by nodes 1 and 3, respectively) are successful. The other nodes, not involved in the collision, listen to the channel activity until the end of the RTS transmissions, and then also start their DIFS timers. Thus after

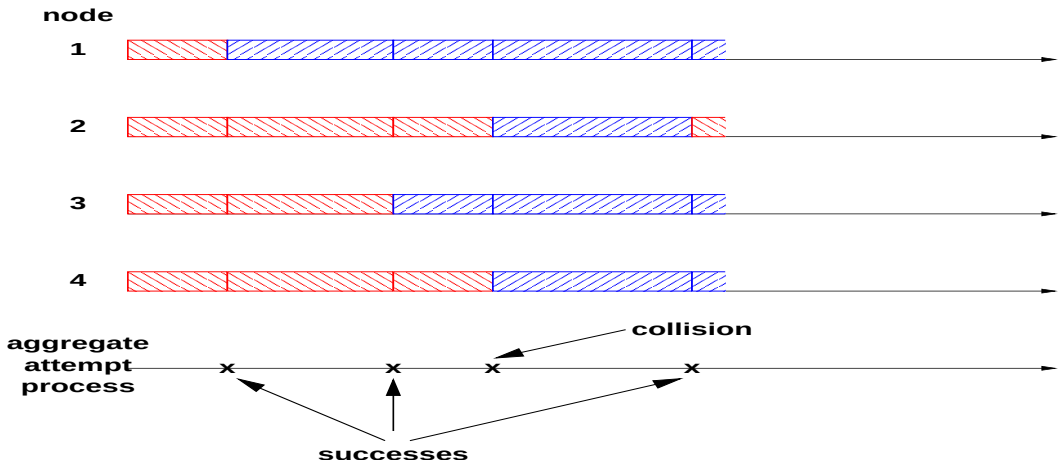

Figure 3: After removing the channel activity from Figure 2 only the back-offs remain. These determine the scheduling of channel access. At the bottom is shown the aggregate attempt process on the channel, with three successes and one collision.

a collision all nodes resume their back-off phases after an amount of time equal to the transmission time of an RTS plus a DIFS.

If attempts to send the packet at the head-of-the-line (HOL) meet with several successive failures, this packet is discarded. By our assumption of saturated queues, there is always another packet waiting to be sent by the upper layers: either the same packet or the next one in line.

We see from the figure that when any node has reserved the channel or whenever there is a collision, all other nodes freeze their back-off timers. We also notice that the evolution of the channel activity after an attempt is deterministic. It is either the time taken for a transmission or for a collision. If there is a transmission then the time depends on which node captures the channel. The latter dependence comes about because the transmission time of a packet depends on the transmission rate and hence on the transmitting node.

Since all nodes freeze their back-offs during channel activity, the total time spent in back-off up to any time t, is the *same* for every node. With this observation, let us now look at Figure 3 which shows the back-offs of Figure 2 with the channel activity removed. Thus in this picture "time" is just the cumulative back-off time at each node. In the IEEE 802.11 standard the back-offs are multiples of the slot time. A success occurs if a single back-off ends at a slot boundary, and a collision occurs when two or more back-offs end at a slot boundary. The nodes could have different back-off parameters (the mean back-off intervals, how these are varied in response to collisions and successes, and the number of retries of a packet). It is clear, however, that the (random) sequence in which the nodes seek turns to access the channel and whether or not each such attempt succeeds depends only on the

back-off process shown in Figure 3. It is therefore sufficient to analyse the back-off process in order to understand the channel allocation process. The saturation assumption is crucial here since, with this assumption, we do not have to take care of any external packet arrivals that may occur during channel activity periods.

Thus, in summary, we can delete the channel activity periods, and we are left with a "conditional time" which we will call *back-off time*. We will analyse the back-off process conditioned on being in back-off time. It will then be shown how this analysis can be used to yield the desired performance measures over all time.

2.2 A Key Approximation

Throughout the rest of the paper *we assume that all the nodes use the same back-off parameters*. Hence the back-off process shown in Figure 3 is symmetric over the nodes. We call this the **homogeneous case** to distinguish it from the **nonhomogeneous** case in which different nodes may use different back-off parameters, as, for example, proposed in the IEEE 802.11e standard (see [8]).

In Figure 3 we also show the aggregate sequence of successes and collisions. In general, this is a complex process, and it is also clear that the success and collision processes of the various nodes are coupled and strongly correlated. In Section 8 we will describe an exact Markov chain model for the joint backoff process of the nodes, but this model is analytically intractable. The following key approximation is made in [3].

The Decoupling Approximation: Let β denote the long run average back-off rate (*in back-off time*) for each node. By the fact that all nodes use the same back-off parameters, and by symmetry, it is assumed that all nodes achieve the same value of β. Let there be n contending transmitters, and consider a given node. The key approximation is to assume that the aggregate attempt process of the other $(n-1)$ nodes is independent of the back-off process of the given node. In IEEE 802.11 the back-off evolves over slots, hence a discrete time model (embedded at slot boundaries) can be adopted. Then the approximation says that if the attempt rate per node is β attempts per slot ($0 \leq \beta \leq 1$), then from the point of view of the given node the number of attempts by the other nodes in successive slots are i.i.d. Binomial random variables with parameters $(n-1)$ and β. It might be expected that such a decoupling approximation should work well when there is a large number of transmitters accessing the channel.

3 Analysis of the Back-Off Process

We generalise the back-off behaviour of the nodes, and define the following back-off parameters.

$K :=$ At the $(K+1)$th attempt either the packet succeeds or is discarded

$b_k :=$ The mean back-off duration (in slots) at the kth attempt for a packet, $0 \leq k \leq K$

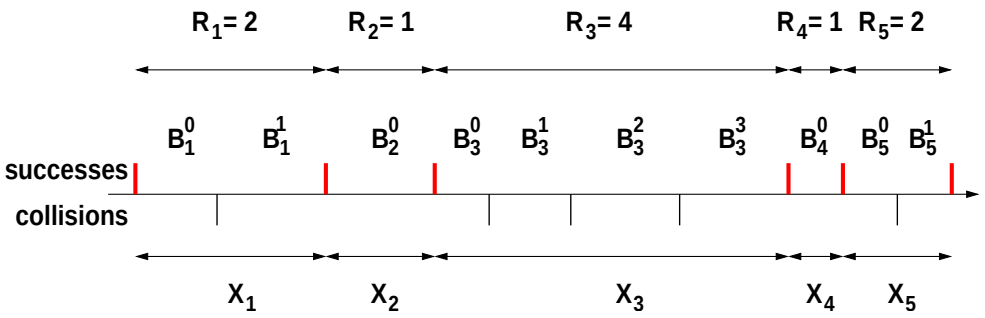

Figure 4: Evolution of the back-offs of a node. Each attempted packet starts a new back-off "cycle."

Since we are limiting ourselves to the homogeneous case, these parameters are the same for all the nodes.

In Figure 4 we show the evolution of the back-off process for a single node. There are R_j attempts until success for the jth packet (no case of a discarded packet is shown in this diagram), and the sequence of back-offs for the jth packet is $B_j^{(i)}, 0 \leq i \leq R_j - 1$. Thus the total back-off for the jth packet is given by

$$X_j = \sum_{i=0}^{R_j - 1} B_j^{(i)}$$

with $\mathsf{E}\left(B_j^{(i)}\right) = b_i$. We observe that the sequence $X_j, j \geq 1$, are renewal life times. Hence, viewing the number of attempts R_j for the jth packet as a "reward" associated with the renewal cycle of length X_j, we obtain from the renewal reward theorem that the back-off rate is given by $\frac{\mathsf{E}(R)}{\mathsf{E}(X)}$.

Now let γ be the collision probability seen by a node, i.e.,

$$\gamma := \mathsf{Pr}\,(\text{an attempt by a node fails because of a collision})$$

Since the back-off behaviour of all the nodes is the same, the collision probability is the same for all the nodes. By the approximation made in Section 2, the successive collision events are independent. It is then easily seen that

$$\begin{aligned} \mathsf{E}(R) &= 1 + \gamma + \gamma^2 \cdots + \gamma^K \\ \mathsf{E}(X) &= b_0 + \gamma b_1 + \gamma^2 b_2 + \cdots + \gamma^k b_k + \cdots + \gamma^K b_K \end{aligned}$$

which yields the following formula for the attempt rate for a given collision probability γ

$$G(\gamma) := \frac{1 + \gamma + \gamma^2 \cdots + \gamma^K}{b_0 + \gamma b_1 + \gamma^2 b_2 + \cdots + \gamma^k b_k + \cdots + \gamma^K b_K}$$

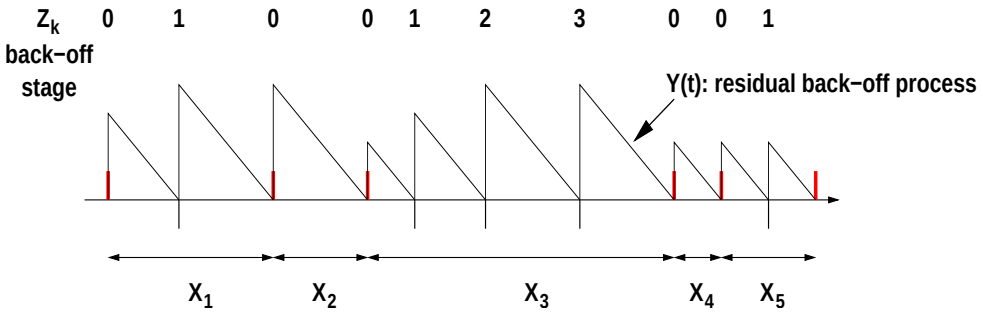

Figure 5: Evolution of the back-off stage (Z_k) and the residual back-off time ($Y(t)$) for the case in which the back-offs are continuous variables.

(1)

Note that, since the back-off times are in slots, the attempt rate $G(\gamma)$ is in *attempts per slot.*

Remarks 3.1

1. Note that the *distribution* of the back-off durations does not matter.
2. Also, observe that the above analysis remains unchanged whether the back-off distributions are discrete (i.e., the back-offs evolve over slots) or are continuous.
3. In the back-off model considered in [3] $K = \infty$; further, there is an $m \geq 1$ such that $b_k = \left(\frac{2^k CW_{\min} \pm 1}{2}\right)$ slots, for $0 \leq k \leq m-1$, and $b_k = \left(\frac{2^m CW_{\min} \pm 1}{2}\right)$ slots, for $k \geq m$. Here $CW_{\min}$ is a positive integer (2^5 in the IEEE 802.11 standard). Substituting these into the expression for $G(\gamma)$ in Equation 1 yields

$$G(\gamma) = \frac{2(1-2\gamma)}{(1-2\gamma)(CW_{\min} \pm 1) + \gamma CW_{\min}(1-(2\gamma)^m)}$$

   attempts per slot, which is the same as in the paper. Note that the $\pm$ alternatives arise depending on whether we take the back-off to be uniformly distributed over $[1, 2, \cdots, CW]$ or over $[0, 1, \cdots, CW-1]$. Evidently, the uniform distribution of back-off durations plays no role in the final results in [3].
4. A more detailed evolution of the back-off process in Figure 4 is shown in Figure 5, where at each time t the residual back-off duration $Y(t)$ is also shown. The process Z_k is the back-off *stage* the node is in. Thus if $K = 7$, $Z_k = 3$, and $Y(t) = 5$, then after 5 time units the current back-off ends. If there is a collision, $Z_k = 4$ and a back-off with mean b_4 is sampled from the specified back-off distribution (uniform in the standard). If $Z_k = 7$ then at the end of the current back-off, irrespective of whether there is a

collision or a success, the next back-off has mean b_0, and is sampled from the specified distribution. It is clear that the process $(Z_k, Y(t))$ is Markov regenerative, with Z_k being the embedded Markov process. It is, however, well known that it is unnecessary to analyse $(Z_k, Y(t))$ to obtain event rates. The process Z_k and the successive back-off intervals constitute a Markov renewal process. It is also well known that for Markov renewal processes event rates and time probabilities are insensitive to distributions of life-times. It should thus be clear why one can directly obtain the formulas above without needing to go through the analysis of the Markov chain in [3], and also why the results are insensitive to the back-off distribution.

4 The Fixed Point Equation

Focusing on the back-off and attempt process of a node, and being given the collision probability γ the attempt rate is provided by $G(\gamma)$ in Equation 1. It is important to recall that in the present discussion all rates are conditioned on being in the back-off periods. Later we will see how to incorporate the channel activity periods. Now if all nodes have the same back-off parameters, they will all see the same average collision probability, γ, and hence will have the same attempt rate. If the attempt rate (or probability) of each node per slot is $\beta, 0 \leq \beta \leq 1$, then, conditioning on an attempt of the given node, the probability of this attempt experiencing a collision is the probability that any of the other nodes attempts in the same slot. Under the decoupling approximation, the number of attempts made by the other nodes is binomially distributed with parameters β and $n-1$. Under the approximation, the number of attempts in successive form an i.i.d. sequence. The probability of collision of an attempt by a node is given by

$$\Gamma(\beta) \quad := \quad 1 - (1-\beta)^{(n-1)} \tag{2}$$

We will show later in the paper that under a certain asymptotic regime the aggregate attempt rate $n\beta$ converges to a positive value as $n \to \infty$. Then (motivated by the binomial to Poisson convergence theorem) for a large number of nodes, it is reasonable to model the attempt process of the other nodes (with respect to a given node) as a sequence of i.i.d. batches (at slot boundaries) with the batch distribution being Poisson with mean $(n-1)\beta$. The collision probability under this model is then clearly given by

$$\Gamma(\beta) \quad := \quad 1 - e^{-(n-1)\beta} \tag{3}$$

It is now natural to expect that the equilibrium behaviour of the system will be characterised by the solutions of the following fixed point equation

$$\gamma \quad = \quad \Gamma(G(\gamma)) \tag{4}$$

If this equation can be solved it will yield the collision probability, from which the attempt rate can be obtained using Equation 1. We will see in Section 6 that throughputs can be obtained once these quantities are determined.

When faced with a fixed point formulation, several questions need to be asked.

1. **Existence and uniqueness:** While fixed points can usually be shown to exist, they may not be unique. Existence of multiple fixed points may suggest multistability, i.e., the system may exist in one of several operating states for long periods of time. Often at least one of these operating states has poor performance; see, for example, [1] and [5] for an example of bistability in circuit switched networks with adaptive routing. We will provide conditions for the uniqueness of the fixed point.

2. **Computation of the fixed point:** If the function $\Gamma(G(\gamma))$ is a contraction then the *fixed point iteration*, i.e.,
$$\gamma_{k+1} = \Gamma(G(\gamma_k))$$
will converge starting from any $\gamma_0 \in [0,1]$. As is often the case, we do not have the contractive property. The following *relaxed* fixed point iteration may work with an appropriate choice of $\alpha \in (0,1)$
$$\gamma_{k+1} = (1-\alpha)\Gamma(G(\gamma_k)) + \alpha\gamma_k$$
The choice of α that leads to convergence will, in general, depend on parameters of the problem. We will examine this technique for the special case in which $K = \infty$ in Section 7.1. For finite K, the numerical results provided in the paper are obtained by using the solve() function in MATLAB.

3. **Convergence of the *system* to the fixed point in some sense:** Even when a fixed point exists and is unique it is not immediately clear in what way the steady state system performance will be related to the quantities obtained from the fixed point. One needs to show that the system dynamics converge in some sense and appropriate quantities in the limit satisfy the fixed point equation. Such an analysis may also lead to a justification of the assumptions that lead to the fixed point equation (e.g., the Poisson and independence assumption in the present paper). See [5] for an example of such an analysis. A related analysis in the context of packet switching systems has been done in [10]. We will defer this issue for our future investigations. In the present paper we proceed assuming that the steady state system behaviour will correspond to the unique fixed point.

4. **Analysis of the fixed point to understand system performance:** The fixed point equation can be analysed to characterise the fixed point and thus obtain quantitative and qualitative results about steady state system performance. The major part of this paper is devoted to such an analysis.

5 Analysis of the Fixed Point Problem

Since $\Gamma(G(\gamma_k))$ is a composition of continuous functions it is continuous. We thus have a continuous mapping from $[0,1]$ to $[0,1]$. Hence by Brouwer's fixed point theorem there exists a fixed point in $[0,1]$. We next turn to uniqueness.

Lemma 5.1 *$G(\gamma)$ is non-increasing in γ if $b_k, k \geq 0$, is a non-decreasing sequence.*

Proof: See the Appendix.

Theorem 5.1 *$\Gamma(G(\gamma)) : [0,1] \rightarrow [0,1]$, has a unique fixed point if $b_k, k \geq 0$, is a non-decreasing sequence.*

Proof: Since $\Gamma(\beta)$ is non-decreasing in β and, by Lemma 5.1, $G(\gamma)$ is non-increasing in γ, it follows that $\Gamma(G(\gamma))$ is non-increasing in γ. The fixed point must therefore be unique, since multiple fixed points will lead to a contradiction to the non-increasing property of $\Gamma(G(\gamma))$. ■

Remark: We observe that in the IEEE 802.11 standard the sequence b_k is non-decreasing. Hence for the practical system there will be a unique fixed point.

5.1 Examples of the Fixed Point Solution

In Figure 6, we show plots of $\Gamma(G(\gamma))$ vs. γ for several parameters. The back-off is expanded multiplicatively with multiplier $p = 2$, as in the IEEE 802.11 standard. In the plot on the top we use the value $K = 7$ which corresponds to the *retry limit* in the standard. In both the plots the initial mean back-off b_0 is 16 slots. The intersection of these plots with the "y=x" line corresponds to the fixed point. We see that the collision probability increases with an increasing number of nodes. For $n \geq 30$, with $K = 7$, the collision probability is larger than with $K = 100$. The collision probability for $n \leq 20$ does not appear to be sensitive to K for $K \geq 7$.

As an illustration, in Figure 7 we show fixed points for some "bad" back-off adaptations. The retry limit is 2 in both the plots, the number of nodes is 20. In the plot on the top a collision causes the back-off to be reduced by a factor of .01. We see that there is a fixed point very near to 1, i.e., a collision probability of 1, implying very poor performance. In the plot on the bottom the initial back-off is also adapted *inversely* with the collision probability (i.e., $b_0 = \frac{10}{\gamma}$), and in addition the back-off is reduced by a factor of .01 when there is a collision. There are now two fixed points, one with a collision probability close to zero, implying an idle network, and the other with a collision probability close to 1 implying that all attempts are wasted. With this, obviously bad, back-off adaptation one can expect bi-stability between two very poorly performing regimes. These contrived examples have been included to serve as a caution that attempts to modify the back-off mechanism have to be made with care.

5.2 Comparison with an *ns2* Simulation

It was reported in [3] that the fixed point analysis works well for IEEE 802.11 parameters. In Figure 8 we demonstrate this by plotting the collision probability obtained from the fixed point method and from an *ns2* simulation.

In all the *ns2* simulations presented in this paper we have used *ns2* version 2.26. The bugs present in the IEEE 802.11 code were patched by using an updated version of the code

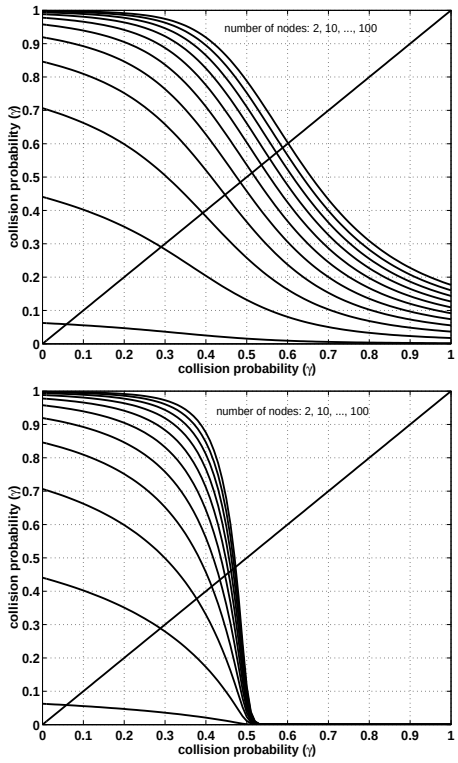

Figure 6: Plots of $\Gamma(G(\gamma))$ vs. γ for two values of K (7 (top) and 100 (bottom)), $b_0 = 16$ slots, and multiplicatively increasing b_k with multiplier $p = 2$. For each K, plots are shown for number of nodes $n = 2, 10, 20, 30, 40, 50, 60, 70, 80, 90, 100$.

taken from the *ns2* snapshot dated January 5, 2004. Static routing was implemented by using *NOAH* code (dated November 2003), downloaded from the web site of J. Widmer, EPFL, (http://icapeople.epfl.ch/widmer/uwb/ns-2/noah/index.html).

As can be seen, the fixed point analysis provides a good approximation for a wide range of values of the number nodes.

6 Calculating Throughputs

Having obtained the collision probability γ and the attempt rate per node β (during back-off periods), we now turn to the problem of calculating the throughputs. In order to do this we first make two key observations.

The first is demonstrated by Figure 9. Because of the i.i.d. batch binomial assumption on the aggregate attempt process, the instants at which a successful transmission or a collision

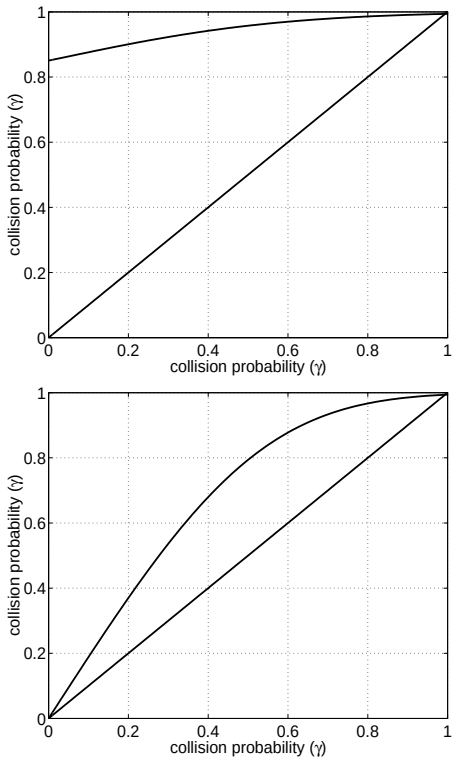

Figure 7: Plots of $\Gamma(G(\gamma))$ vs. γ for $K = 2$, and multiplicatively increasing b_k with multiplier $p = .01$. In the plots on the top $b_0 = 10$ slots, and in the plots on the bottom $b_0 = \frac{10}{\gamma}$ slots. For each case, plots are shown for number of nodes $n = 20$.

ends are renewal instants. Each such instant is followed by a time until the next attempt, followed by a collision or a success, and so on.

The second observation is that since all the nodes follow the same back-off process, each node has an equal probability of winning the allocation "race." With this in mind we can now discard the back-off times and focus only on the times when an attempt is made and on the intervening channel activity. A successful attempt leads to the channel being allocated to one of the n contending nodes with equal probability. Hence in a saturated system, in order to compute the amount of time the channel will be allocated to a node, we only need to know the identity of the packet that will be found at the head-of-the-line if the channel is allocated to the node.

Consider the model shown in Figure 10. The nodes are visited in random order with equal probability. Each node receives an *open loop* stream of packets. There are m_i streams

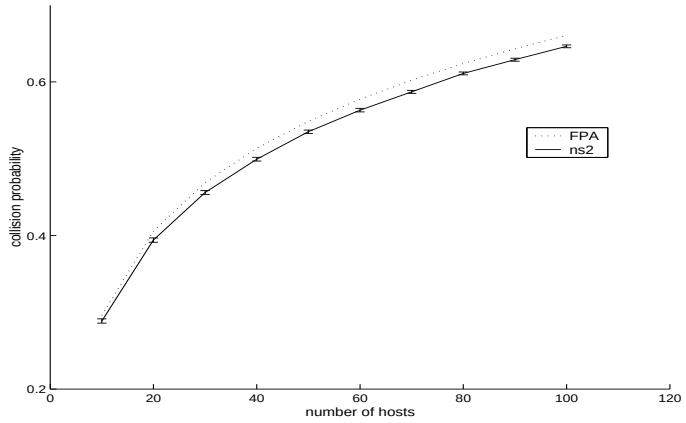

Figure 8: Plot of collision probability versus number of nodes. Comparison of collision probability (γ) obtained from an *ns2* simulation (plot labeled *ns2*), and the fixed point analysis (plot labeled *FP*). 95% confidence intervals are shown for the values obtained from the *ns2* simulation. In the *ns2* simulation the default IEEE 802.11 parameters are used: see Remarks 3.1, paragraph 3, with $K = 6$ and $m = 5$; the data rate is 11 Mbps and the control packet rate is 2 Mbps.

being handled by node i. These are indexed by $1 \leq j \leq m_i$; these would represent m_i flows from node i to some of the other nodes. We can thus use the term "flow (i, j)".

By "open-loop" we mean that packets arrive to the node and have to be delivered; there are no acknowledgement and flow control as in TCP controlled traffic. A fraction $p_{i,j}$ of the

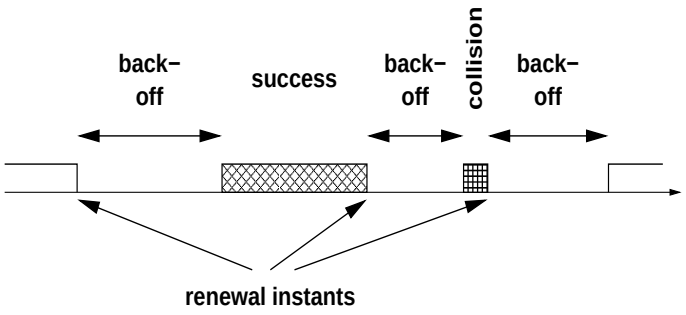

Figure 9: The aggregate process of back-offs and channel activity

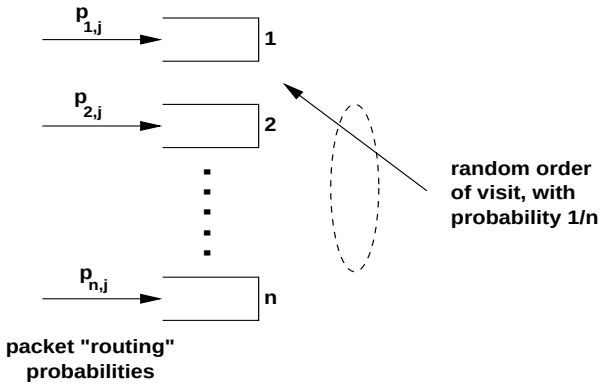

Figure 10: The n transmitters are served in random order with equal probability for each node.

packets at node i belong to stream $j, 1 \leq j \leq m_i$. Since the node is saturated there is always a packet at the head-of-the-line when the channel is allocated to any node, and $p_{i,j}$ is the probability that the packet is from flow j. Let us define the packet length of flow (i,j) to be $L_{i,j}$ and the physical transmission rate for flow (i,j) to be $C_{i,j}$ *bits per slot.*

In addition, we define,

$T_o :=$ is the fixed overhead with a packet transmission in slots (e.g., IEEE 802.11b: $T_o = 90.8$ slots)

$T_c :=$ is the fixed overhead for an RTS collision in slots (e.g., IEEE 802.11b: $T_c = 17$ slots)

The above two observations, the traffic model described above, and the parameters listed above, lead immediately to the expression in Equation 5 for the saturation throughput of flow (i,j) (in bits per slot) given the collision probability γ and the per node attempt rate β.

$$\theta_{i,j}(\beta) = \frac{\frac{\beta(1-\beta)^{n-1}}{1-(1-\beta)^n} p_{i,j} L_{i,j}}{\frac{1}{1-(1-\beta)^n} + \sum_{i=1}^{n} \left(\frac{\beta(1-\beta)^{n-1}}{1-(1-\beta)^n} \left(\left(\sum_{k=1}^{m_i} p_{i,k} \frac{L_{i,k}}{C_{i,k}} \right) + T_o \right) \right) + \left(\frac{(1-(1-\beta)^n - n\beta(1-\beta)^{n-1})}{1-(1-\beta)^n} T_c \right)} \quad (5)$$

The formula follows from the renewal reward theorem. The mean renewal time (see Figure 9) is the mean time until an attempt, plus the mean time for channel activity; i.e., a transmission or a collision. The term $\frac{1}{1-(1-\beta)^n}$ is the mean time until an attempt and assumes that the aggregate attempt process is binomial. When there is an attempt the

channel is allocated to node i (with probability $\frac{\beta(1-\beta)^{n-1}}{1-(1-\beta)^n}$), else there is a collision, for which the channel will be busy for the time T_c. If the channel reservation succeeds, then the head-of-the-line packet at node i is of flow (i,j) with probability $p_{i,j}$, and transmitting this takes the time $\frac{L_{i,j}}{C_{i,j}} + T_o$. The mean reward during the cycle is $\frac{\beta(1-\beta)^{n-1}}{1-(1-\beta)^n} p_{i,j} L_{i,j}$, thus yielding the displayed expression. Canceling the term $1-(1-\beta)^n$, the formula simplifies to the expression in Equation 6.

$$\theta_{i,j}(\beta) = \frac{\beta(1-\beta)^{n-1} p_{i,j} L_{i,j}}{1 + \sum_{i=1}^{n} \left(\beta(1-\beta)^{n-1} \left(\left(\sum_{k=1}^{m_i} p_{i,k} \frac{L_{i,k}}{C_{i,k}}\right) + T_o\right)\right) + \left((1-(1-\beta)^n - n\beta(1-\beta)^{n-1})\ T_c\right)} \tag{6}$$

6.1 Low Speed Transmitters Bound All Throughputs

It has been observed (see, for example, [2]) that when there are several flows with different physical transmission rates then the throughput of all the flows is bounded by the slowest transmission rate. We can examine this observation using Equation 6.

If 2 nodes i_1 and i_2 are such that for some $j_1, 1 \leq j_1 \leq m_1$, and $j_2, 1 \leq j_2 \leq m_2$

$$p_{i_1,j_1} L_{i_1,j_1} = p_{i_2,j_2} L_{i_2,j_2}$$

then it follows from Equation 6 that

$$\theta_{i_1,j_1}(\gamma,\beta) \leq \min\{C_{i_1,j_1}, C_{i_2,j_2}\}$$

and

$$\theta_{i_2,j_2}(\gamma,\beta) \leq \min\{C_{i_1,j_1}, C_{i_2,j_2}\}$$

i.e., the flow with the lower physical rate will bound the throughput of both.

Remark: The above analysis points to an important observation. Suppose we are interested in achieving flow throughputs that are proportional to their physical link rates; i.e., $\theta_{i,j} = \nu C_{i,j}$ for some ν. It has been suggested in previous literature that this can be achieved by appropriately choosing the packet lengths. We notice from Equation 6 that the desired throughput proportionality can be achieved only be making $L_{i,j}$ proportional to $\frac{C_{i,j}}{p_{i,j}}$, which requires knowledge of the $p_{i,j}$s, which may not be practicable.

Let us now consider a simpler situation with n nodes each being the transmitter for a single flow and all packet lengths being equal to L. Then the *total* network throughput is given by

$$\Theta(\beta) = \frac{n\beta(1-\beta)^{n-1} L}{1 + \sum_{i=1}^{n} \left(\beta(1-\beta)^{n-1} \left(\frac{L}{C_i} + T_o\right)\right) + \left((1-(1-\beta)^n - n\beta(1-\beta)^{n-1})\ T_c\right)} \tag{7}$$

Since the denominator is bounded below by $\sum_{i=1}^{n}\left(\beta(1-\beta)^{n-1}\left(\frac{L}{C_i}+T_o\right)\right)$, it can be seen that

$$\Theta(\beta) \leq \frac{1}{\frac{1}{n}\sum_{i=1}^{n}\frac{1}{C_i}} \leq n \times \min_{1\leq i\leq n} C_i$$

i.e., *the total network throughput is bounded above by the reciprocal of the harmonic means of the physical bit rates of the n flows.* Thus, for example, if there are two flows with physical rates 2 Mbps and 4 Mbps then the total network throughput will be bounded by $\frac{2}{\frac{1}{2}+\frac{1}{4}} = 2.667$ Mbps. Also, with equal packet lengths, we see that this total throughput is shared equally among all the flows.

7 An Asymptotic Analysis

We motivate a study of asymptotics with the plots in Figure 11. We notice that the fixed points appear to be converging, and there is not much variation in them for $K \geq 15$. In fact, for $n \leq 20$, there is little change in the fixed point even for $K \geq 7$. The reason for this is clear. The collision probability is small for these small values of n, and hence the retry limit K is rarely reached; increasing K beyond some value ceases to have any additional effect. Another inference we can make from these plots is that for large n, $K = 7$ gives a rather large collision probability. This may suggest that one should actually use a larger value of K in practice, say 10 or 15. This will not change the performance for small n and would improve the performance for large n.

Thus we are motivated to analyse the fixed point for $K \to \infty$. Such an asymptotic analysis can be expected to yield closed form results that will provide information even for K as small as 15. A similar asymptotic analysis has also been carried out independently by Kwak et al in [7]; while their final results are the same as our Theorem 7.2, we have displayed an analytical form for the fixed point solution (see Theorem 7.1), and we derive our asymptotic results by taking a limit in this solution. Further, we also provide a relaxed fixed point iteration for computing the fixed point (see Section 7.1).

To permit closed form analysis, let us take $b_0 = b$ slots, and $b_k = p^k \times b_0$, where $p \geq 1$; hence, by Theorem 5.1, a unique fixed point still exists. The multiplicative increase is in any case a part of the IEEE 802.11 standard; we are generalising to an arbitrary multiplier in order to study the impact of the value of this multiplier.

Assuming $\gamma < \frac{1}{p}$, and taking $K \to \infty$, we see that

$$G(\gamma) \quad = \quad \frac{1}{b_o} \times \frac{1-p\gamma}{1-\gamma}$$

Note that the assumption that $\gamma < \frac{1}{p}$ does not affect the fixed point analysis presented earlier, since we will see in Theorem 7.2 that the fixed point in the limit $K \to \infty$ is less than $\frac{1}{p}$.

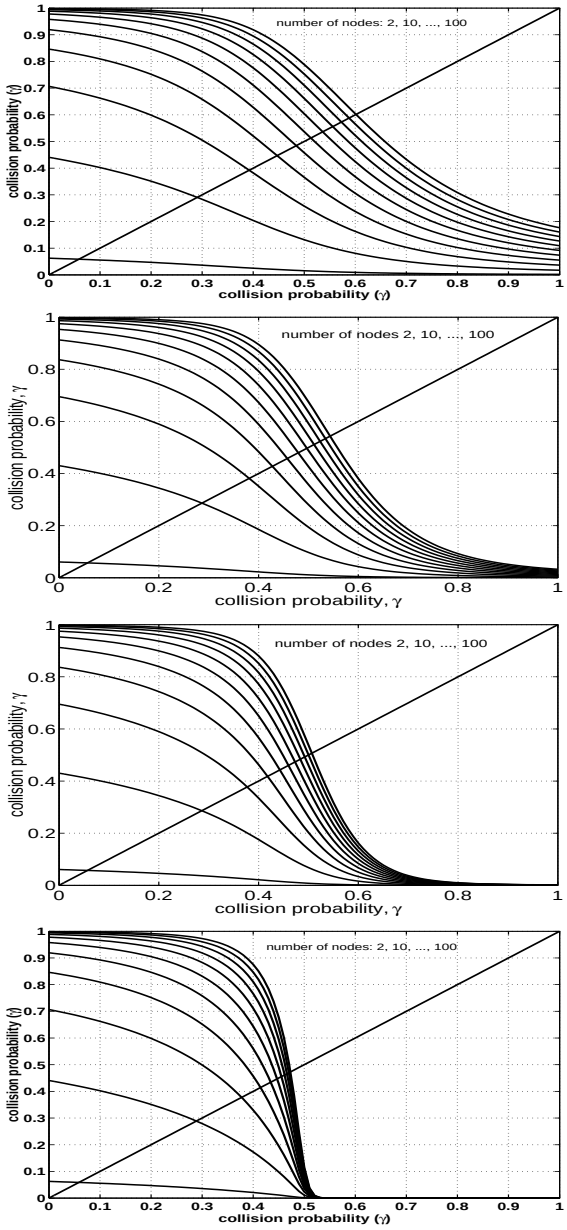

Figure 11: The variation of the fixed points for $K = 7$ (top panel), $K = 10$ (second panel), $K = 15$ (third panel), and $K = 100$ (bottom panel); $b = 16$, $p = 2$, and the number of nodes $n = 2, 10, 20, 30, 40, 50, 60, 70, 80, 90, 100$.

Given γ, $G(\gamma)$ is the probability of attempt of any node. Then using the batch Poisson version of the collision probability in Equation 3, the fixed point equation becomes

$$\gamma = 1 - e^{\left((n-1)\times\frac{1}{b_0}\times\frac{1-p\gamma}{1-\gamma}\right)} \quad (8)$$

In order to obtain compact expressions, let us define

$$\eta = \frac{n-1}{b_0}$$

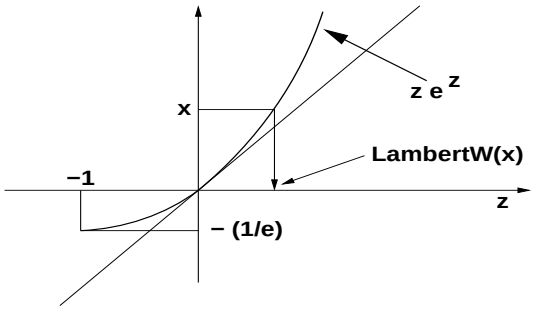

Figure 12: The LambertW function is the inverse function of ze^z; notice that for $x \geq -\frac{1}{e}$, $LambertW(x) \leq x$, with equality only for $x = 0$.

Theorem 7.1 *The fixed point is of the form* $\gamma(\eta) = \frac{LambertW(\eta(p-1)e^{\eta p})-\eta(p-1)}{LambertW(\eta(p-1)e^{\eta p})}$.

Remark: For $x \geq -\frac{1}{e}$, $LambertW(x)$ is defined as the inverse of the function ze^z; see Figure 12.

Proof: We proceed from Equation 8. Writing $\nu = 1 - \gamma$, and using the definition of η, this equation can be rewritten as

$$\nu = e^{-\eta p} e^{\frac{\eta(p-1)}{\nu}}$$

Multiplying both sides by $\eta(p-1)$, we obtain

$$\eta(p-1)e^{\eta p} = \frac{\eta(p-1)}{\nu} e^{\frac{\eta(p-1)}{\nu}}$$

It follows from the definition of $LambertW(\cdot)$ that

$$\frac{\eta(p-1)}{\nu} = LambertW(\eta(p-1)e^{\eta p})$$

from which the result follows by substituting $1 - \gamma$ for ν. ■

7.1 A Relaxed Fixed Point Iteration

The fixed point $\gamma(\eta)$ can only be computed numerically. In this section we provide a relaxed fixed point iteration. With reference to Equation 8, let us define the function

$$f(\gamma) := 1 - e^{\left((n-1)\times\frac{1}{b_0}\times\frac{1-p\gamma}{1-\gamma}\right)}$$

and, with $\gamma_0 := \frac{1}{p}$, consider the sequence of values generated by the iterations

$$\gamma_{k+1} = (1-\alpha)f(\gamma_k) + \alpha\gamma_k \tag{9}$$

where $0 < \alpha < 1$. Notice that $\alpha = 0$ corresponds to the usual fixed point iteration, which will converge if $f(\gamma)$ is a contraction. The above iteration is called a *relaxed* fixed point iteration. We will now provide a condition on α that will ensure that the iterates converge to the fixed point.

First of all, since $f(\gamma)$ is continuous, it is clear from the iteration in Equation 9 that if the sequence of iterates converge then they must converge to the fixed point. It is also clear that if, for each k, $\gamma_k \geq f(\gamma_k)$ then the sequence $\{\gamma_k\}$ is nonincreasing. This follows because

$$\gamma_{k+1} = (1-\alpha)f(\gamma_k) + \alpha\gamma_k \leq \gamma_k$$

if and only if

$$f(\gamma_k) \leq \gamma_k$$

Thus, since $\gamma_k \geq 0$, for the convergence of the sequence $\{\gamma_k\}$ it suffices to ensure that $\gamma_k \geq f(\gamma_k)$ for all k.

Now, it can easily be shown that the derivative of $f(\gamma)$ at $\gamma = \frac{1}{p}$ is given by $D := -\frac{n-1}{b_0}\frac{p^2}{p-1}$, and that, for $\gamma_{k+1} \leq \gamma_k$

$$f(\gamma_{k+1}) - f(\gamma_k) \leq |D|\ (\gamma_k - \gamma_{k+1})$$

From this inequality we can see that to ensure $f(\gamma_k) \leq \gamma_k$, for all k, it is sufficient to ensure that, for all k,

$$|D|\ (\gamma_k - \gamma_{k+1}) \leq \gamma_{k+1} - f(\gamma_k)$$

Using the iteration in Equation 9 this is equivalent to ensuring that, for all k,

$$|D|(1-\alpha)(\gamma_k - f(\gamma_k)) \leq \alpha(\gamma_k - f(\gamma_k))$$

Hence it suffices that

$$|D|(1-\alpha) \leq \alpha$$

or that

$$\alpha \geq \frac{|D|}{|D|+1}$$

Thus, for example, with $n = 10$ nodes, $b_0 = 16$ slots, and $p = 2$, it relaxed fixed point iteration with α such that $\frac{2.25}{3.25} < \alpha < 1$ will yield the unique fixed point $\gamma(\eta)$.

7.2 Taking n to ∞

We now wish to take n to ∞ and study the limit of the fixed point solution obtained in Theorem 7.1. For this we need the following properties of the LambertW function. The proof is provided in the Appendix.

Lemma 7.1

1. For $a > 0$,
$$\lim_{x \to \infty} \frac{LambertW(axe^x)}{x} = 1 \tag{10}$$
2. For $0 < a \leq 1$, $LambertW(axe^x) \leq x$
3. For $0 < a < 1$, the convergence in Equation 10 is from below.

The following result is now obtained by applying Lemma 7.1 to the expression for γ in Theorem 7.1.

Theorem 7.2

1. $\gamma(\eta) < \frac{1}{p}$
2. $\lim_{n \to \infty} \gamma(\eta) \uparrow \frac{1}{p}$
3. $\lim_{n \to \infty} n\beta \uparrow \ln(\frac{p}{p-1})$

Remarks 7.1

1. Theorem 7.2 provides explicit expressions for the collision probability and the fixed point for large K and a large number of nodes. We have already discussed above (recall Figure 11) that K only needs to be larger than 15 for the large K asymptotics to apply. Thus we see that for large n the collision probability is directly related to the back-off multiplier p, and is the reciprocal of this multiplier.
2. We also see that $n\beta$, the mean attempt rate per slot, goes to $\ln(\frac{p}{p-1})$, and hence the attempt probability per node (during back-off periods) behaves like $O(\frac{1}{n})$. This lends some support to the original assumption that from the point of view of a node the attempt process of the other nodes can be viewed as an independent process with i.i.d. batch Poisson arrivals in successive slots.

7.3 Asymptotic Aggregate Throughput

Let us now consider n nodes handling n flows with all the flows having the same transmission rate, C. The aggregate throughput of the network is given by (compare with Equation 7)

$$\Theta(\beta) = \frac{n\beta e^{-n\beta} L}{1 + \left(n\beta e^{-n\beta}\left(\frac{L}{C} + T_o\right)\right) + \left((1 - e^{-n\beta} - n\beta e^{-n\beta})\ T_c\right)}$$

We infer from this equation that, as $n \to \infty$ the aggregate throughput converges to

$$\tau(p) := \frac{(1 - \frac{1}{p})L}{\frac{1}{\ln(\frac{p}{p-1})} + \left((1 - \frac{1}{p})(\frac{L}{C} + T_o) + \left(\frac{\frac{1}{p}}{\ln(\frac{p}{p-1})} - (1 - \frac{1}{p})\right) T_c\right)}$$

The following result is then immediately obtained

Theorem 7.3 *1.* $\lim_{p\to\infty} \tau(p) = 0$

2. $\lim_{p\to 1} \tau(p) = 0$

3. $\tau(p)$ *is maximised at*

$$p = \frac{\frac{T_c}{T_c+1}}{LambertW\left(-\frac{1}{e} \cdot \frac{T_c}{(T_c+1)}\right) + \frac{T_c}{T_c+1}}$$

Remarks 7.2

1. The behaviour of the aggregate throughput as p goes to its two extremes is as expected. If $p \to 1$ then the nodes do not increase their back-off intervals in response to collisions. The collision probability becomes large and the throughput drops to 0. Obviously, as $p \to \infty$ collisions cause a drastic reduction in attempts essentially shutting the nodes off.

2. In an attempt see what the above asymptotic results have to say about realistic network parameters, in Figure 13 we plot the aggregate throughput for finite K and finite n, using the formula in Equation 7 with equal transmission rate for all the flows. We see that the throughput increases steeply for $1 < p < 2$, but is quite flat with p after $p = 2$. There is an optimal value of p, but unless p is very close to 1, the throughput is not very sensitive to p. It can be seen that the back-off multiplier used in the standard, i.e., $p = 2$, is adequate unless the number of nodes becomes very large. For $T_c = 17$ (slots), the third part of Theorem 7.3 returns $p = 3.85$, which compares well with the curve for $n = 60$ in Figure 13.

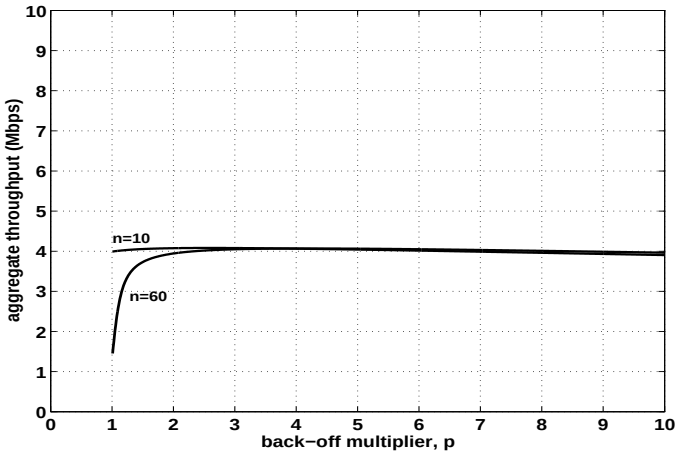

Figure 13: Aggregate throughput plotted vs. the back-off multiplier p for two values values of n. The network parameters are $K = 10$, $b_0 = 16$ slots, data packet length 8000 bits, packet overhead 592 bits, slot time 20 μs, transmission rate for all flows 11 Mbps, fixed (rate independent) data packet transmission overhead 52 slots, collision overhead 17 slots.

8 Comparison with a DTMC Model of the Back-Off Process

The previous sections dealt with the following points: characterisation of the solution of the fixed point equation; analysis of system performance assuming that the system operates at the fixed point; asymptotic analysis of the fixed point as $n \to \infty$; numerical validation of the performance results obtained from the fixed point analysis in comparison with a discrete event simulation model. In this section we turn to the important issue of the relationship between an exact DTMC model of the coupled back-off processes and the fixed-point analysis. We proceed with the following assumptions:

- The number of nodes $n \geq 2$
- K is the retry limit
- b_0 is the initial back-off, *expressed as a multiple of the slot time.*
- Exponential back-off with multiplier $p > 1$, i.e., $b_k = p^k b_0, 1 \leq k \leq K$.
- Back-off durations are geometrically distributed, or, equivalently, when a node is in back-off stage k, it attempts in the next slot with probability $\frac{1}{b_k}$.

The n nodes all use the same back-off parameters. We focus only on the cumulative back-off time, since, as argued in Section 2.1, the evolution of the back-off process is what determines channel access to the nodes. With this in view, we index the slots during the system back-off time by $t = 0, 1, 2, \cdots$.

For the system with n nodes, at the beginning of slot t (more precisely at time $t+$), let, for $1 \leq j \leq n$, $S_j^{(n)}(t)$ $(\in \{0, 1, 2, \cdots\})$ denote the back-off stage of node j; i.e., if $S_j^{(n)}(t) = k$, then node j will make an attempt at $t+1$ with probability $\frac{1}{b_k}$. If node j attempts at $t+1$ and there is a collision then $S_j^{(n)}(t+1) = k+1$, otherwise there is a success and $S_j^{(n)}(t+1) = 0$. If the node does not make an attempt at $t+1$ (with probability $1 - \frac{1}{b_k}$) then $S_j^{(n)}(t+1) = S_j^{(n)}(t) = k$. Let $\mathbf{S}^{(n)}(t)$ denote the vector of the nodes' back-off states at t. It is clear that $\mathbf{S}^{(n)}(t)$, $t = 0, 1, 2, \cdots$, is a Markov chain on $\{0, 1, \cdots, K\}^n$.

The dimensionality of the Markov chain $\mathbf{S}^{(n)}(t)$, $t = 0, 1, 2, \cdots$ grows with n. It is therefore more convenient to work with the process that counts the number of nodes in each back-off stage. This will be a $K+1$ dimensional process for any number of nodes. To this end, given a state $\mathbf{s} \in \mathrm{Z}^{+n}$ of the process $\mathbf{S}^{(n)}(t)$, define the number of nodes in the back-off stage k to be

$$M_k^{(n)}(t) = \sum_{j=1}^{n} I_{\{s_j = k\}}$$

where $I_{\{\cdot\}}$ denotes the indicator of the set $\{\cdot\}$. Let $\mathbf{M}^{(n)}(t)$ denote the vector random process $M_k^{(n)}(t), k \in \mathrm{Z}^+$. From the foregoing, it is clear that $\mathbf{M}^{(n)}(t)$ is a Markov process taking values in the set

$$\mathcal{M}^{(n)} := \{\mathbf{m} : m_k \text{ nonnegative integers}; \sum_{k=0}^{K} m_k = n\}$$

The following Lemmas will be used to establish that for $b_0 > 1$, and $p > 1$, the DTMC $\mathbf{M}^{(n)}(t)$ is irreducible over the state space $\mathcal{M}^{(n)}$. For two states $\mathbf{m}_1$ and $\mathbf{m}_2$ in $\mathcal{M}^{(n)}$ we write $\mathbf{m}_1 \rightarrow \mathbf{m}_2$ to denote that $\mathbf{m}_2$ is *reachable* from $\mathbf{m}_1$, i.e., starting in state $\mathbf{m}_2$ the DTMC reaches state $\mathbf{m}_1$ in a finite number of steps with positive probability.

Lemma 8.1 *For $b_0 > 1$, and $p > 1$, for all $\mathbf{m} \in \mathcal{M}^{(n)}$, $\mathbf{m} \rightarrow (n, 0, 0, \cdots, 0)$.*

Remark: This result asserts that from any state in $\mathcal{M}^{(n)}$ the state in which all the nodes are in the initial back-off stage is reachable.

Proof: Since $b_0 > 1$ and $p > 1$, for every $k, 1 \leq k \leq K$, $b_k > 1$, i.e., the attempt probability of a node in any back-off stage is less than 1. Then starting from any state $\mathbf{m} \in \mathcal{M}^{(n)}$ the state $(n, 0, 0, \cdots, 0)$ can be reached if exactly one node among the nodes in the stages $1, 2, \cdots, K$ attempts in $m_1 + m_2 + \cdots + m_K$ successive slots, and hence succeeds. In each successive slot the number of nodes in back-off stage 0 increases by 1. This has positive probability. ■

Lemma 8.2 *For $b_0 > 1$, and $p > 1$, for all $\mathbf{m} \in \mathcal{M}^{(n)}$, $(n, 0, 0, \cdots, 0) \rightarrow \mathbf{m}$.*

Proof: See the Appendix. ■

The above two lemmas immediately yield the following result.

Theorem 8.1 *For $b_0 > 1$, and $p > 1$, the DTMC $\mathbf{M}^{(n)}(t)$ on $\mathcal{M}^{(n)}$ is irreducible.* ■

It follows that under the conditions $b_0 > 1$ and $p > 1$, the DTMC $\mathbf{M}^{(n)}(t)$ is positive recurrent. Let $\boldsymbol{\pi}^{(n)}$ denote the stationary probability measure on $\mathcal{M}^{(n)}$.

For small values of K (e.g., 1 or 2) $\boldsymbol{\pi}^{(n)}$ can be numerically computed. Now given $\boldsymbol{\pi}^{(n)}$, the collision probability γ can be obtained as shown in Equation 11, where we have assumed that $b_k > 1$ for all k. For a given $\mathbf{m} \in \mathcal{M}^{(n)}$, in the next slot, the number of attempts by nodes in the kth back-off stage can be no more than m_k.

$$\gamma = \frac{\displaystyle\sum_{\{\mathbf{m}\in\mathcal{M}^{(n)}\}} \sum_{\{\mathbf{a}\le\mathbf{m}:\sum_{i=0}^{K} a_i \ge 2\}} \left(\boldsymbol{\pi}^{(n)}(\mathbf{m}) \times \sum_{i=0}^{K} a_i \times \left(\Pi_{k=0}^{K} \binom{m_k}{a_k} \left(\frac{1}{b_k}\right)^{a_k} \left(1-\frac{1}{b_k}\right)^{(m_k-a_k)} \right) \right)}{\displaystyle\sum_{\{\mathbf{m}\in\mathcal{M}^{(n)}\}} \sum_{\{\mathbf{a}\le\mathbf{m}:\sum_{i=0}^{K} a_i \ge 1\}} \left(\boldsymbol{\pi}^{(n)}(\mathbf{m}) \times \sum_{i=0}^{K} a_i \times \left(\Pi_{k=0}^{K} \binom{m_k}{a_k} \left(\frac{1}{b_k}\right)^{a_k} \left(1-\frac{1}{b_k}\right)^{(m_k-a_k)} \right) \right)} \tag{11}$$

Denote such an attempt vector by $\mathbf{a}$. Thus for given $\mathbf{m}$, we have $\mathbf{0} \le \mathbf{a} \le \mathbf{m}$. Then it is easily seen that in this expression the denominator is the total rate of attempts, and the numerator is the total rate of collisions. Note the terms $\sum_{i=0}^{K} a_i$, since we need to count all the attempts or collisions in each slot.

A natural question to ask is whether the collision probability yielded by the above Markov chain is well approximated by the fixed point analysis. Sample results are shown in Table 1. Results are shown for $K = 1$ and $K = 2$. Two values of b_0 are examined: $b_0 = 16$, and also $b_0 = 2$. It can be seen that the fixed point analysis approximates the collision probability very well.

A further exploration of the relationship between the exact Markov model and the fixed-point analysis is a subject of our ongoing research.

9 Application to the Analysis of TCP Controlled File Transfers

It is well known that over 90% of the traffic in the Internet is generated by what are essentially file transfers between computers. All common applications such as e-mail, ftp, and web browsing basically involve no more than the transfer of files between one or more computers. Such file transfers are elastic in the sense that no guaranteed transfer rate

No. of Nodes	DTMC ($K=1$)	FPA ($K=1$)	DTMC ($K=2$)	FPA ($K=2$)
1	0.0598	0.0592	0.0595	0.0587
2	0.1111	0.1105	0.1088	0.1078
3	0.1568	0.1563	0.1510	0.1500
4	0.1983	0.1979	0.1879	0.1870
5	0.2365	0.2362	0.2209	0.2202
6	0.2720	0.2718	0.2508	0.2502
7	0.3052	0.3050	0.2782	0.2778
8	0.3363	0.3362	0.3036	0.3033
9	0.3657	0.3656	0.3272	0.3270
10	0.3933	0.3933	0.3494	0.3493
11	0.4196	0.4195	0.3703	0.3702
12	0.4444	0.4444	0.3900	0.3900
13	0.4680	0.4680	0.4088	0.4088
14	0.4905	0.4905	0.4266	0.4266
15	0.5119	0.5119	0.4436	0.4436
16	0.5323	0.5323	0.4598	0.4599
17	0.5518	0.5518	0.4754	0.4755
18	0.5703	0.5703	0.4903	0.4904
19	0.5881	0.5881	0.5046	0.5048
1	0.3889	0.3904	0.3333	0.3398
2	0.5944	0.5956	0.4929	0.4987
3	0.7273	0.7277	0.6036	0.6074
4	0.8159	0.8159	0.6864	0.6886
5	0.8757	0.8756	0.7505	0.7517
6	0.9162	0.9160	0.8010	0.8015
7	0.9436	0.9434	0.8412	0.8412
8	0.9621	0.9620	0.8732	0.8730
9	0.9745	0.9745	0.8988	0.8986
10	0.9829	0.9829	0.9194	0.9190
11	0.9886	0.9886	0.9358	0.9355
12	0.9924	0.9924	0.9489	0.9487
13	0.9949	0.9949	0.9595	0.9592
14	0.9966	0.9966	0.9678	0.9676
15	0.9977	0.9977	0.9745	0.9744
16	0.9985	0.9985	0.9798	0.9797
17	0.9990	0.9990	0.9840	0.9840
18	0.9993	0.9993	0.9874	0.9873
19	0.9995	0.9995	0.9900	0.9900

Table 1: Collision probabilities obtained from the DTMC and from fixed point analysis (FPA) for $K = 1$ and $K = 2$. The table on the top is for $b_0 = 16$ and the one at the bottom is for $b_0 = 2$.

is required, and, furthermore, the rate can vary during an ongoing transfer. Thus the transfer rates can adapt to the time-varying number of active connections in the network. In the Internet, such adaptation is carried out by the adaptive window mechanisms of TCP. When there is network congestion (indicated by packet loss, or specially marked bits in acknowledgement (ACK) packets) the TCP transmitter reduces its window, thus reducing the transfer rate. The default behaviour of the sender is to gradually increase the window, up to a maximum value, say, $W_{\max}$. In this section we are interested in using the analysis developed thus far in the paper to obtain formulas for the throughput of TCP controlled file transfers rates over an IEEE 802.11 WLAN.

9.1 Some Modeling Assumptions

We will make the following assumptions:

A1 The files are infinitely long. Thus we do not deal with web transfers. Practically, this assumption means that our analysis applies to large file transfers, such as software, document, or media downloads.

A2 The modulation scheme and bit rate of the physical connection between a pair of communicating wireless devices is ideally adapted (but fixed) so that there is no packet loss owing to bit errors. Further, the retransmission time-out at each TCP transmitter is large enough so that time-outs never takes place.

A3 At the transmitter of each wireless device the capacity of the buffer is such that there is no packet loss. This assumption effectively holds in practice if the number of file transfer connections through a node is small enough so that the sum of the maximum TCP windows of all the connections is less than the buffer size. For, say, 10 connections, this would typically require a buffer of no more than 512 KB.

A4 The file transfer throughputs are bottlenecked only by the rates they obtain over the WLAN. For example, the transfers could be between the wireless devices across an ad hoc WLAN, or, in the infrastructure case, between the wireless devices and devices attached to a high speed wired LAN to which the AP is attached. For transfers within a building or campus this assumption is practically valid since most wired LANs are based on 100 Mbps to 1 Gbps Ethernet.

Owing to Assumption A1 it makes sense to talk about the long run time average throughput of a transfer. From Assumptions A2 and A3 it follows that the TCP window of each connection grows to its maximum value, and by Assumption A4, each data packet or ACK of all the TCP connections will be queued at the transmitter of one of the WLAN devices.

Let us adopt the following connection model. There are m connections, indexed by $j, 1 \leq j \leq m$. The source node of connection j is denoted by $s(j)$, and the receiver node is denoted by $r(j)(\neq s(j))$. Thus, for connection j, the TCP ACKs will queue up at the transmitter of node $r(j)$. The data packet length for connection i is denoted by L_j and the

ACK packet length by $L_j^{(ack)}$. In general, each node will transmit data packets for some connections and ACK packets for other connections.

In order to use the "saturated queues" analysis presented earlier in the paper, we make the following additional assumption

A5 The configuration of the TCP connections and the sizes of their windows are such that the transmitter queues of the wireless devices never empty out.

Remark: This assumption is made to permit us to use the fixed point analysis presented earlier in the paper. It, however, considerably restricts the scenarios to which the analysis will apply. For example, the common situation of two or more devices simultaneously downloading files via an AP is not covered by our analysis. This is because the AP needs to send many more packets for each packet that each of the devices sends, and hence the device queues will empty out, violating our saturated queues assumption.

We will utilise Assumption A5 as follows. Recall our discussion in Section 6. If all the n queues always have packets to send, then they always contend for the channel, and each successful attempt "belongs" to each of the queues with equal probability, $\frac{1}{n}$.

9.2 A Formula for Connection Throughput

Let us now focus only on the successful attempt instants. Such a success belongs to node i with probability $\frac{1}{n}$. The HOL packet at that node is then transmitted. If this packet is of length L and the transmission rate is C then a time $\frac{L}{C} + T_o$ elapses. If the packet transmitted is a data packet then possibly an ACK is inserted into the transmitter queue of the receiving node (note that if delayed ACKs are used then not every data packet causes an ACK to be generated). On the other hand, if the packet transmitted is an ACK packet then one or more packets are inserted into the transmitter queue of the receiving node. *Thus the queues can be viewed as evolving only at successful polling instants.* This is an important observation as it allows us to ignore the back-off periods while analysing the evolution of the packet queues. Note that this observation does not hold if there are finite rate open-loop arrival processes into the nodes, as these arrival processes will cause the queues to evolve even during back-off periods.

From the above observations, we can now proceed by analysing the discrete time random polling model shown in Figure 14. The discrete "time" in this model evolves over packets. Note that we do not need to be concerned with packet lengths (data or ACK), or physical bit rates. We will see that all we need from this model is the fraction of polls to a queue that find packets of each type at the head-of-the-line. There are several TCP connections modeled as "chains" or classes of customers circulating between pairs of nodes. The populations of the chains are the TCP window sizes. If the delayed ACK threshold for a connection is greater than 1 (let us say 2), then at the receiving node for that connection 2 data packets give rise to one ACK packet. We can view this ACK packet as being a batch of 2, that is served together.

The state of the random polling model is the position and type of each packet in each queue. This process evolves over packet times. It is easy to see that the evolution of

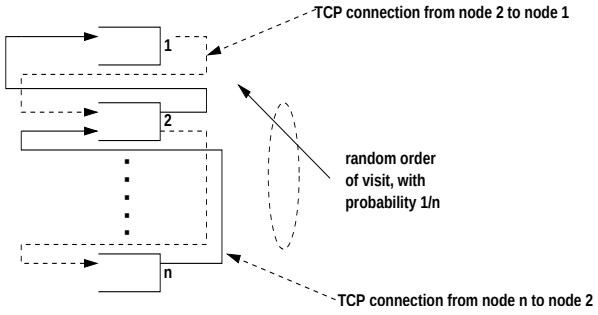

Figure 14: There are several TCP connections, modeled as "chains" of customers with a fixed population (the window size) circulating in a random polling network. The solid arrows between the queues show the direction of TCP data transfer for a connection, and the dashed arrows show the direction of TCP ACK transmission. The n transmitters are served in random order with equal probability for each node.

this rather complicated process is Markovian. Analysis of this Markov chain will yield the following probabilities, that will be used in the throughput formulas.

$h_{i,j}$: the probability that at a polling instant the HOL packet at node i is a data packet from connection j

$h_{(i,j)}^{(ack)}$: the probability that at a polling instant the HOL packet at node i is an ACK packet for connection j (for which node i is the receiver node, i.e., $i = r(j)$)

By the observations made just before these definitions, we can conclude that *the probabilities $h_{i,j}$ and $h_{(i,j)}^{(ack)}$ do not depend on data and ACK packet lengths, nor on the physical bit rates of the connections.* These probabilities will depend only on the maximum TCP window sizes, the delayed ACK thresholds, and the connection configurations (i.e., which nodes carry which connections). We also note that once we have these probabilities, the throughput of connection j can be immediately obtained as in Equation 12 (see also Equation 6), where (γ, β) are obtained from the fixed-point analysis.

$$\theta_j(\beta) = \frac{\beta(1-\beta)^{n-1} h_{s(j),j} L_j}{1 + \sum_{i=1}^{n} \beta(1-\beta)^{n-1} \left(\left(\sum_{\{j:s(j)=i\}} h_{i,j} \frac{L_j}{C_{i,r(j)}} + \sum_{\{j:r(j)=i\}} h_{i,j}^{(ack)} \frac{L_j^{(ack)}}{C_{i,s(j)}} \right) + T_o \right) + (1 - (1-\beta)^n - n\beta(1-\beta)^{n-1}) T_c} \quad (12)$$

This formula has the same form as the one in Equation 6. In the numerator the term $\beta(1-\beta)^{n-1}$ is the probability that node $s(j)$ has a success, $h_{s(j),j}$ is the probability that the

HOL packet belongs to connection j, and when both these events occur connection j has a "reward" of L_j bits. The denominator is the mean length of a back-off and and attempt cycle.

Remarks 9.1

1. To be technically correct Equation 12 should have been obtained as the ratio of two expectations with respect to the stationary distribution of the Markov chain describing the random polling model. We have shown only the final result in terms of the HOL probabilities at the polling instants, as this is simple and intuitively clear.
2. In Equation 6 the HOL probabilities were obtained from the ratios of the open-loop arrival rates into the queues. In Equation 12, however, the HOL probabilities will need to be obtained from the packet level analysis of the random polling model shown in Figure 14. We will show how this is done in the next subsection.
3. The denominator of the expression now includes a term for the service provided to TCP ACKs.
4. We have used the fact that all data packets within TCP connection j have the same length L_j, and the ACK packets within TCP connection j have the same size $L_j^{(ack)}$. If this were not the case then we would need to make a more elaborate definition of the HOL probabilities which would have to include the probability of finding packets of each possible length.

9.3 Obtaining the HOL Probabilities

Let λ_j be the throughput of connection j through its sender node $s(j)$ in the random polling model shown in Figure 14. Thus λ_j the average number of packets of connection j that pass through the node $s(j)$ per packet served in the polling model.

Theorem 9.1 *If at each success instant one of the nodes is polled with equal probability (i.e., we have the model in Figure 14) then* $h_{s(j),j} = \lambda_j n$.

Proof: Let $\pi_{s(j),j}$ denote the fraction of packet services in the model of Figure 14 during which the HOL position at node $s(j)$ is occupied by a data packet of connection j. Since the mean time that a packet spends in the HOL position is n, by Little's Theorem we have

$$\pi_{s(j),j} = \lambda_j n$$

Owing to random polling, the HOL position at node $s(j)$ is observed by a Bernoulli process with probability of "success" equal to $\frac{1}{n}$. Hence by the result that Bernoulli "arrivals" see time averages, we can conclude that

$$h_{s(j),j} = \pi_{s(j),j} = \lambda_j n$$

■

Remarks 9.2

1. If the throughput of ACKs for connection j through its receiver node $r(j)$ is $\lambda_j^{(ack)}$ then by the same argument as in Theorem 9.1 it follows that

$$h_{s(j),j}^{(ack)} = \lambda_j^{(ack)} n$$

2. We note that the hypothesis of the Theorem 9.1 that "at each success instant one of the nodes is polled with equal probability" requires the saturation assumption, i.e., Assumption A5, to hold. There are TCP connection configurations for which this assumption will not hold. For example consider a single TCP connection from Node 1 to Node 2. The TCP receiver uses a delayed ACK threshold of 2; i.e., it returns one ACK for two received data packets. Clearly over a large number of packet transmitted we cannot say that about half will come from Node 1 and the other half from Node 2. In this case the receiver node will tend to empty out and the saturation assumption will not apply. On the other hand if Node 2 was also sending to Node 1 then our analysis will apply.

3. In view of Theorem 9.1 we need to analyse the random polling model and obtain the λ_js and the $\lambda_j^{(ack)}$s, and this will yield the HOL probabilities needed in the throughput formula.

9.4 Comparison with *ns2* Simulations

In Figure 15 we compare the results from the analysis presented above and *ns2* simulations; 95% confidence intervals are shown around the simulation results. For comments on the version of *ns2* used, see Section 5.2. The scenario simulated is that there are n nodes paired up with n other nodes; each node in the first group is performing a TCP controlled long file transfer to its corresponding member in the other group. The maximum receiver window for each TCP connection is 20 packets, the TCP packet length is 1 KB, and the receivers do not delay the ACKs (i.e., an ACK is returned for each received data packet). In this situation, of course, $h_{i,j}$ will be 1 whenever Node i is the source node of connection j, and $h_{i,j}^{ack}$ will be 1 whenever Node i is the receiver node for connection j. The physical link rates are all 11 Mbps. The aggregate throughput over all the connections is plotted vs. the number of connections. We notice that the match between analysis and simulations is good, with the worst case error being about 6%. The simulation trace file showed that during the simulations there was no TCP time-out; thus our Assumption A2 held in this case.

Another scenario that we evaluated was two nodes sending files to each other, simultaneously. In this case the aggregate throughput predicted by the model is 2.4164 Mb/s,

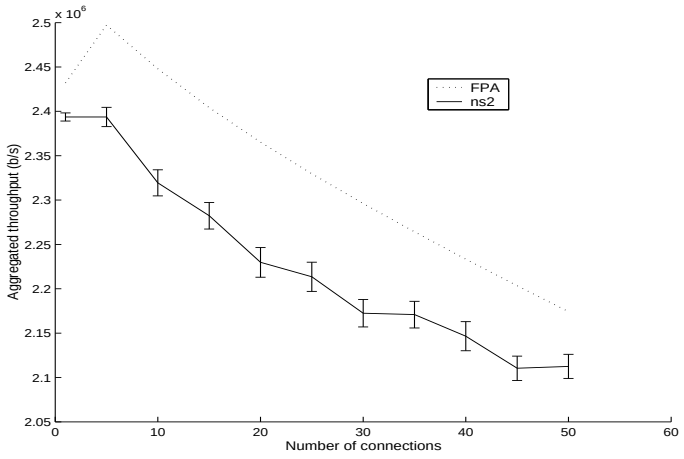

Figure 15: Plot of aggregate TCP controlled file transfer throughput vs. number of simultaneous transfers over an IEEE 802.11b network. Results obtained from the approximate analysis in the paper and from *ns2* simulations are shown. We show 95% confidence intervals around the simulation results. In the *ns2* simulation the IEEE 802.11 parameters are used; the data rate is 11 Mbps and the control rate (used to send RTS, CTS and ACK) is 2 Mbps.

while *ns2* simulations return a 95% confidence interval of [2.4054,2.4153] Mb/s. In the simulation, the throughput obtained by each transfer is approximately a half of the aggregate throughput.

10 Summary

In this paper we begin by providing a simplification and generalisation of a saturation throughput analysis of single cell IEEE 802.11 WLANs as provided by Bianchi [3]. We first focus on the back-off process which is analysed via a decoupling assumption and the solution of a fixed point equation. Our analysis provides a simple and general representation of the fixed point equation. The representation is insensitive to the distribution of the back-off times. We show that if the mean back-off durations for successive retrials are monotone nondecreasing then the fixed point equation has a unique solution. Then we provide general throughput formulas for open-loop arrival processes (e.g., UDP transfers). We recover the observation that connections with small physical rates dominate the throughputs of other connections. In fact, we show that in a simple case the network throughput is bounded by the reciprocal of the harmonic mean of the physical layer transmission rates.

We then turn to the special case of exponential back-off with an arbitrary positive multiplier, p, and where we do not limit the number of retrials a node can make. This leads to simpler expressions which permit us to study the network performance as the number of nodes goes to infinity. For this case, we obtain a characterisation of the fixed point solution for the collision probability for each n. Then we take n to ∞ and obtain the limit of the collision probability and aggregate attempt rate that agree with the results of Kwak et al in [7]. We also provide a relaxed fixed point iteration for computing the fixed point for any finite n when the number of retrials is not limited. The asymptotic aggregate throughput is obtained and from this the optimal back-off multiplier p is also derived.

For exponential back-off, and geometrically distributed back-off periods, the back-off process can be modeled via a discrete time Markov chain. We study this DTMC, and for some simple computable cases we compare the collision probability obtained from the DTMC with that obtained from the fixed point analysis.

Finally, we show how the saturation throughput analysis can be used to obtain TCP controlled file transfer throughputs for some network scenarios. In this analysis we exploit the idea that for window controlled traffic the back-off process evolution can be decoupled from the packet service process, the latter being modeled by a random polling queue.

Our analysis in this paper still leaves open several avenues for future work. Even for the saturated node case we have not taken care of the important physical phenomenon of *capture* which, owing to the use of direct sequence spread spectrum communication, could be significant for a small number of contending nodes. The fixed point analysis needs to be extended to nonhomogeneous nodes, i.e., the situation in which nodes use different back-off parameters, as would arise with IEEE 802.11e networks. Some extensions to the fixed point analysis in the homogeneous case and some results on the fixed point analysis for the nonhomogeneous case are provided in our companion paper [9]. Finally, the saturation assumption needs to be relaxed in order to permit the modeling of arbitrary open-loop arrival processes, or of general TCP transfer scenarios where the loads on the nodes are not balanced.

11 Appendix

Proof: (Lemma 5.1)
We have

$$G(\gamma) \quad := \quad \frac{1+\gamma+\gamma^2\cdots+\gamma^K}{b_0+\gamma b_1+\gamma^2 b_2+\cdots+\gamma^k b_k+\cdots+\gamma^K b_K}$$

and we need to show that the derivative of this function with respect to γ is negative. Taking the derivative we find that we need to show that

$$\sum_{k=0}^{K} b_k\gamma^k\left(\sum_{j=1}^{K} j\gamma^{(j-1)}\right) \leq \sum_{k=0}^{K}\gamma^k\left(\sum_{j=1}^{K} j b_j\gamma^{(j-1)}\right)$$

i.e.,

$$\sum_{k=0}^{K}\sum_{j=1}^{K} j b_k \gamma^{(k+j-1)} \leq \sum_{k=0}^{K}\sum_{j=1}^{K} j b_j \gamma^{(k+j-1)}$$

or, equivalently, we need to show that

$$\sum_{n=1}^{2K} \gamma^{(n-1)} \sum_{\substack{j=\max\{(n-K),1\} \\ k=(n-j)}}^{\min\{n,K\}} j(b_j - b_k) \geq 0$$

Now we consider each term $\sum_{\substack{j=\max\{(n-K),1\} \\ k=(n-j)}}^{\min\{n,K\}} j(b_j - b_k)$ and show that it is non-negative. To this end, define

$$m(n) = |\{(j,k) : j + k = n, 1 \geq j, k \leq K\}|,$$

where $|\cdot|$ denotes set cardinality. Then we can rewrite the previous expression as

$$\sum_{j=\max\{(n-K),1\}}^{\max\{(n-K),1\}+\lfloor \frac{m}{2} \rfloor - 1} ((n-j)-j)\,(b_{n-j} - b_j) + n(b_n - b_0) 1_{\{1 \leq n \leq K\}}$$

which is non-negative since, in the range of the sum, $(n-j) - j \geq 0$ and $b_{n-j} - b_j \geq 0$. ■

Proof: (Theorem 7.1) This is just a simple manipulation of the fixed point equation to get it into the form of the LambertW function. The fixed point equation is

$$\gamma = 1 - e^{\left((n-1) \times \frac{1}{b_0} \times \frac{1-p\gamma}{1-\gamma} \delta\right)}$$

which can be rewritten as

$$(1-\gamma) = e^{-\eta p} e^{\frac{\eta(p-1)}{(1-\gamma)}}$$

This expression can be rearranged as follows

$$\eta(p-1)\; e^{\eta p} = \frac{\eta(p-1)}{(1-\gamma)}\; e^{\frac{\eta(p-1)}{(1-\gamma)}}$$

It follows, from the definition of the LambertW function (and utilising the fact that $p > 1$) that

$$\frac{\eta(p-1)}{(1-\gamma)} = LambertW(\eta(p-1)\; e^{\eta p})$$

The result follows by rearranging the equation to extract γ. ■

Proof: (Lemma 7.1)

1. For $x \geq 0$, write $z(x) = LambertW(axe^x)$, i.e.,

$$z(x) e^{z(x)} = axe^x$$

It is easily seen that for $x > 0$, $z(x) > 0$, and $z(x) \uparrow \infty$ for $x \to \infty$. Now, taking natural logarithms, we obtain, for all $x > 0$,

$$\ln z(x) + z(x) = \ln ax + x$$

or

$$\frac{z(x)}{x} = \frac{\frac{\ln ax}{x} + 1}{\frac{\ln z(x)}{z(x)} + 1}$$

which, on taking $x \to \infty$ yields the desired result since $\frac{\ln ax}{x}$ and $\frac{\ln z(x)}{z(x)}$ both go to 0.

2. By definition, $LambertW(xe^x) = x$, and LambertW is monotone increasing for positive arguments. Hence, for $0 < a \leq 1$, $LambertW(axe^x) \leq x$.

3. Follows by combining the previous two parts. ■

Proof: (Theorem 7.2) Observe that we can write $LambertW(\eta(p-1)e^{\eta p})$ as $LambertW(\frac{p-1}{p}\eta p e^{\eta p})$, with $\frac{p-1}{p}$ being less than 1, by virtue of $p > 1$. The first two parts now follow upon using Lemma 7.1 in

$$\gamma(\eta) = \frac{LambertW(\eta(p-1)e^{\eta p}) - \eta(p-1)}{LambertW(\eta(p-1)e^{\eta p})}$$

The limit for $n\beta$ is obtained as follows. We have

$$(1-\gamma) = e^{-(n-1)\beta\delta}$$

Rearranging we have

$$(n-1)\beta = \frac{-\ln(1-\gamma)}{\delta}$$

It follows that

$$n\beta \quad = \quad \frac{n}{n-1}(n-1)\beta \uparrow_{n\to\infty} \frac{1}{\delta}\ln(\frac{p}{p-1}) \quad \blacksquare$$

Proof: (Lemma 8.2) Three cases arise depending on $\mathbf{m}$

(i) $m_K \geq 2$

(ii) There exists $j', 1 \leq j' \leq K$, such that $m_{j'-1} \geq 2$

(iii) There exists $j', 1 \leq j' \leq K$, such that $\sum_{k=j'}^{K} m_k = 1$

Case (i): The sequence of transitions
$(n, 0, 0, \cdots, 0) \to (m_0, \sum_{k=1}^{K} m_k, 0, \cdots, 0) \to (m_0, m_1, \sum_{k=2}^{K} m_k, 0, \cdots, 0) \to$
$\cdots \to (m_0, m_1, m_2, \cdots, m_K)$ has positive probability. The successive transitions correspond

to $\sum_{k=j}^{K} m_k \geq 2, 1 \leq j \leq K$, nodes attempting together and hence colliding, while the other nodes do not attempt. Each such transition results in the colliding nodes increasing their back-off stage by 1, until the desired state $(m_0, m_1, m_2, \cdots, m_K)$ is reached.

Case (ii): This is the same as Case (i) except that we stop at the state $(m_0, m_1, m_2, \cdots, m_{j'-1}, 0, \cdots, 0)$.

Case (iii): In this case $\mathbf{m}$ is of the form $(m_0, m_1, m_2, \cdots, m_{j'-1}, 0, 0, m_l, 0, 0)$ where $m_l = 1$ for some $l, j' \leq l \leq K$. There are two subcases here.

(a) $m_0 \geq 1$

(b) $m_0 = 0$

Subcase (iii-a): Consider the following transitions $(n, 0, 0, \cdots, 0) \rightarrow (m_0 - 1, \sum_{k=1}^{K} m_k + 1, 0, \cdots, 0) \rightarrow (m_0 - 1, m_1, \sum_{k=2}^{K} m_k + 1, 0, \cdots, 0) \rightarrow \cdots \rightarrow (m_0 - 1, m_1, m_2, \cdots, m_{j'-1} + 2, 0, \cdots, 0) \rightarrow (m_0 - 1, m_1, m_2, \cdots, m_{j'-1}, 0, 0, \cdots, 0, 2, 0 \cdots, 0)$ until the "2" reaches stage l. Then one of these nodes in stage l attempts yielding $(m_0, m_1, m_2, \cdots, m_{j'-1}, 0, 0, m_l, 0, 0)$.

Subcase (iii-b): Define $i = \min\{k : 1 \leq k \leq K,\ m_k > 0\}$ and consider the state $(m_i, m_{i+1}, \cdots, m_{j'-1}, 0, 0, m_l, 0, 0, 0, \cdots, 0)$, i.e., a left shift of $\mathbf{m}$ by i. Now consider the transitions in Subcase (iii-a) until this state is reached. Then i more transitions in which all nodes attempt, and hence collide, will yield $\mathbf{m} = (0, 0, \cdots, 0, 0, m_i, m_{i+1}, \cdots, m_{j'-1}, 0, 0, m_l, 0, 0)$.

■

Acknowledgements

We are grateful to Chadi Barakat for sparing his time for some useful discussions.

References

[1] J. M. Akinpelu. The overload performance of engineered networks with non-hiearchical routing. *Bell Sytem Technical Journal*, pages 1261–1281, September 1984.

[2] G. Berger-Sabbatel, F. Rousseau, M. Heusse, and A. Duda. Performance anomaly of 802.11b. In *Proceedings of IEEE Infocom 2003*. IEEE, 2003.

[3] G. Bianchi. Performance analysis of the IEEE 802.11 distributed coordination function. *IEEE Journal on Selected Areas in Communications*, 18(3):535–547, March 2000.

[4] F. Cali, M. Conti, and E. Gregori. IEEE 802.11 protocol: Design and performance evaluation of an adaptive backoff mechanism. *IEEE Journal on Selected Areas in Communications*, 18(9):1774–1780, September 2000.

[5] R. J. Gibbens, P. J. Hunt, and F. P. Kelly. *Bistability in Communication Networks*, chapter in Disorder in Physical Systems, pages 113–128. Oxford University Press, 1990.

[6] Anurag Kumar and Deepak Patil. Stability and throughput analysis of unslotted cdma-aloha with finite numer of users and code sharing. *Telecommunication Systems*, 8:257–275, 1997.

[7] B.-J. Kwak, N.-O. Song, and L. E. Miller. Analysis of the stability and performance of exponential backoff. In *Proceedings of IEEE WCNC*, 2003.

[8] Stefan Mangold, Sunghyun Choi, Peter May, Ole Klein, Guido Hiertz, and Lothar Stibor. IEEE 802.11e wireless LAN for quality of service. In *Proc. European Wireless (EW 2002)*, February 2002.

[9] Venkatesh Ramaiyan, Anurag Kumar, and Eitan Altman. A note on a fixed point analysis of csma/ca wireless lans: Uniqueness, short term unfairness, and ieee 802.11. Manuscript in preparation, May 2004.

[10] A. L. Stolyar. The asymptotics of the stationary distribution of a closed queueing system. *Problems of Information and Transmission*, 25(4):321–331, 1990. Translation of the article in Russian, published in 1989.

Unité de recherche INRIA Sophia Antipolis
2004, route des Lucioles - BP 93 - 06902 Sophia Antipolis Cedex (France)

Unité de recherche INRIA Futurs : Parc Club Orsay Université - ZAC des Vignes
4, rue Jacques Monod - 91893 ORSAY Cedex (France)
Unité de recherche INRIA Lorraine : LORIA, Technopôle de Nancy-Brabois - Campus scientifique
615, rue du Jardin Botanique - BP 101 - 54602 Villers-lès-Nancy Cedex (France)
Unité de recherche INRIA Rennes : IRISA, Campus universitaire de Beaulieu - 35042 Rennes Cedex (France)
Unité de recherche INRIA Rhône-Alpes : 655, avenue de l'Europe - 38334 Montbonnot Saint-Ismier (France)
Unité de recherche INRIA Rocquencourt : Domaine de Voluceau - Rocquencourt - BP 105 - 78153 Le Chesnay Cedex (France)

Éditeur
INRIA - Domaine de Voluceau - Rocquencourt, BP 105 - 78153 Le Chesnay Cedex (France)
http://www.inria.fr
ISSN 0249-6399